

# Flow Structure and Sustainability of Pools in Gravel-bed Rivers

S.E. Parkinson, P. Goodwin<sup>1</sup> & D. Caamaño<sup>2</sup>

*US Bureau of Reclamation, Pacific Northwest Region, Boise Idaho, USA*

<sup>1</sup>*Center for Ecohydraulics Research, University of Idaho, Boise, Idaho, USA*

<sup>2</sup>*Department of Civil Engineering, Universidad Católica de la Santísima Concepción, Concepción, CHILE*

**ABSTRACT:** Pool-riffle channel morphology in gravel-bed streams creates a range of micro-habitats that are important for maintaining ecological diversity. This study is motivated by the need to restore sustainable spawning and over-wintering habitat for salmon as a means of mitigating for dam construction. The velocity reversal hypothesis (Gilbert, 1914, Keller 1971, 1972) has been used as a potential mechanism for the sustainability of pools. Velocity reversal implies that the velocities are smaller through the pool than across the riffle at low and intermediate flows. At high discharges this condition becomes reversed and velocities through the pool may exceed the velocities across the riffle. Recent criteria have been developed that utilize the bathymetric characteristics of the channel to ascertain whether or not velocity reversal will occur. However, it is unclear whether the velocity reversal criterion predicts pool sustainability under all flow conditions and if limitations to this approach exist. The role of a high velocity core in controlling sediment deposition and scour processes was investigated under different flow discharges in addition to conditions when velocity reversal may not recreate the original pool riffle morphology.

The flume results of this study demonstrate that although velocity reversal provides a useful indicator of the persistence of pool features, bed shear stress and sediment flux reversal do not occur at the same discharge or location as the velocity reversal. The study also demonstrated the differential transport capacity through the pool and riffle as well as conditions when these features are lost beyond self-recovery.

## 1 INTRODUCTION

Gravel-bed rivers are an important habitat for salmonids, which are at risk throughout the Northwest region of North America and are the focus of extensive environmental legislation and

litigation. The pool-riffle morphology in gravel-bed rivers is particularly important as the diversity in physical habitat in these reaches is critical for spawning and other life stages (Stanford *et al.*, 2005, Tilman, 1998). The river cross sectional shapes, at any location along the watercourse, are a function of the flow, the quantity and character of the sediment in movement through each section, and the character or composition of the materials making up the bed and banks of the channel (Leopold *et al.* 1964; Knighton, 1998; Federal Interagency Stream Corridor Restoration Working Group, 1998). Pool-riffle sequences are one of the possible river reach morphologies created by these interactions. Many restoration projects attempt to restore pool morphology in a sustainable and minimum maintenance manner.

A number of hypotheses have been presented to explain the formation and self maintenance of pool riffle sequences. The reversal hypothesis has been evaluated with field measurements, laboratory investigations and numerical simulations. The reversal hypothesis defines the condition where a high discharge event creates a higher velocity condition within the pool feature than across the riffle. Reversals in near-bed velocity and shear stress have been more commonly reported. Average cross sectional velocity reversals have been demonstrated to occur under limited conditions (Booker 2001, Thompson 2011). These reversals require that a more rapid increase in cross sectional area with increasing discharge of the riffle relative to the pool has to occur. However, this one dimensional simplification does not fully describe the three dimensional physical processes occurring between the pool and riffle. Recent findings have shown that constriction of flow through the pool, either caused by point bar geometry or effective area reduction due to a recirculating eddy, creates a narrow core of higher velocity water.

This flow convergence was suggested by MacWilliams *et al.*, (2006) as the pool formation mechanism in both free-formed and forced pools. Caamaño *et al.* (2010) further defined this jet structure as comprising velocities greater than 90% of the maximum depth-averaged velocity observed within a cross section. Numerical simulations of this flow structure also illustrated a change in orientation as well as a change in intensity and location of vertical and horizontal eddies. These non-uniform flow effects created by this high velocity core structure have the capacity to influence the local transport and sediment routing dynamics through the pool.

Self maintenance of pool-riffle sequences are dependent on the differential routing and scouring of sediment. In order to assess the response of a pool to sediment pulses during high flows or artificially high sediment loads created by landuse practices or wildfire, it is necessary to measure the differential sediment transport between the pool and riffle. However, this is very difficult and hazardous to do in the field at the high flow conditions when the geomorphically significant

sediment transport is occurring. Therefore, to investigate the sediment transport characteristics of a pool-riffle sequence, a physical model was constructed.

This model facilitated the visualization of physical processes and detailed velocity structure observed in field data and in numerical simulations. This model was built to represent a pool-riffle sequence located on the Red River within the Red River Wildlife Management Area. The purpose of utilizing this specific reach was to validate the results observed in the three-dimensional numerical modeling as well as qualifying the conceptual model processes proposed in the self-maintenance of pool-riffle sequences (Caamaño *et al.*, 2010).

## 2 STUDY SITE

The headwaters of the Red River originate within the Clearwater Mountain Range in north-central Idaho (lat. 45° 45', long. 115° 24'), USA. The Red River joins the American River to become the South Fork Clearwater River. This particular study reach is a meandering gravel-bed channel that flows through an unconfined 4.5 km long meadow situated at an elevation of 1,280 m and bounded by forested mountains (Klein *et al.*, 2007) within the Red River Wildlife Management Area (RRWMA) (Figure 1).

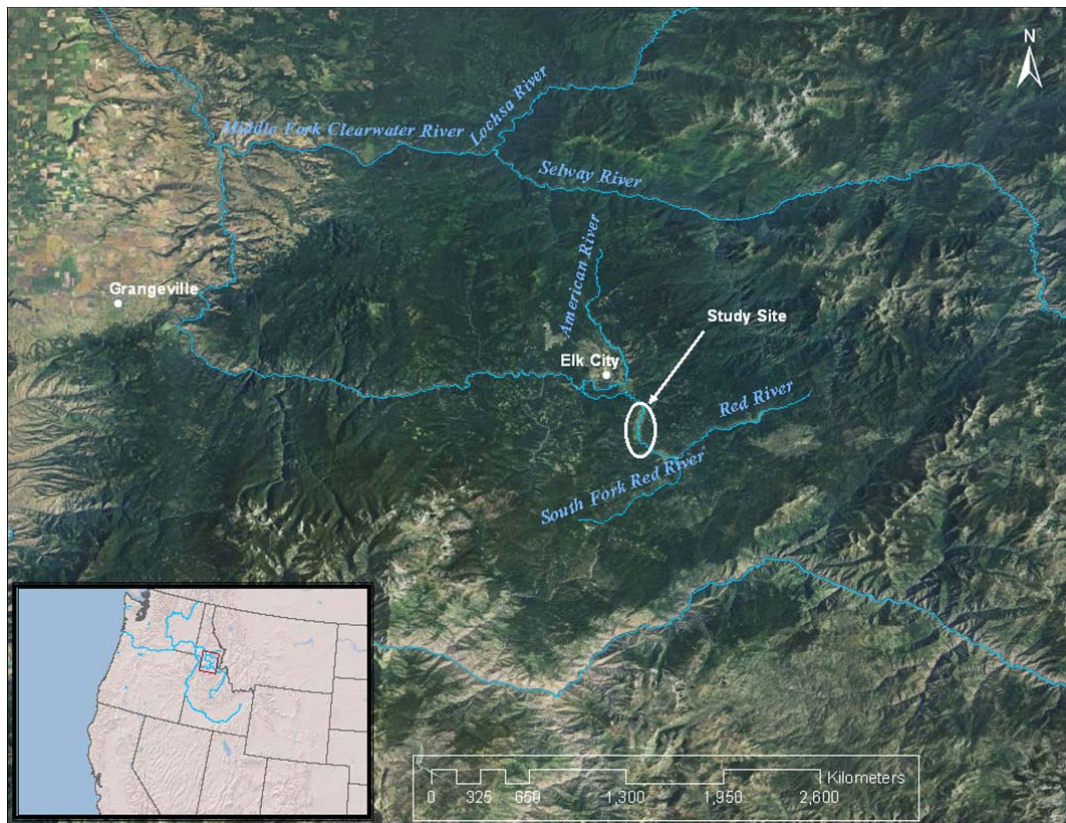


Figure 1. Location of Red River Wildlife Management Area, north central Idaho.

The study site illustrated in Figure 2 is the Lower Red River Meadow where restoration activities were conducted in several reaches starting in 1993. The pool-riffle sequence selected for this study was free formed (not forced by external flow obstructions such as logs or boulders; Montgomery *et al.*, 1995) during the first high flow event immediately after the final restoration phase of the RRRWMA in 2000. For approximately 10 years, the geometry of these features has remained relatively consistent since project completion. This specific pool-riffle sequence is situated downstream of a straight, 50 m long run and curves into a double pool-riffle sequence with bankfull discharge at  $16.62 \text{ m}^3/\text{s}$  and an average bank top width of 11.25 m, before opening to a wider stream section. The upstream run has a symmetrical, almost rectangular cross section that allows a uniform flow distribution in the stream before entering the first pool. The first pool-riffle sequence has a deep residual pool depth followed by a coarse riffle, whereas the second pool is shallower, with a finer-grained riffle (Figure 2 and Table 1). Figure 3 illustrates the first riffle feature at both low flow and high flow conditions.



Figure 2. Location of the study reach (inset) relative to the RRWMA restoration efforts.

Table 1. Grain size distribution, modified from Caamaño *et al.*, (2010).

Bedform:	Pool 1	Riffle 1	Pool 2	Riffle 2
$d_{16}$	12 mm	38 mm	19 mm	26 mm
$d_{50}$	42 mm	65 mm	46 mm	47 mm
$d_{84}$	74 mm	94 mm	82 mm	80 mm
$d_{90}$	82 mm	105 mm	90 mm	85 mm

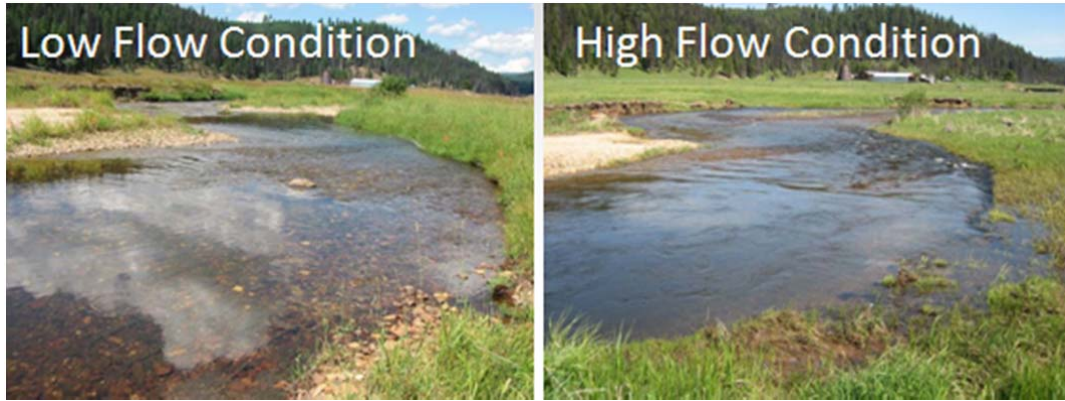


Figure 3. Riffle 1 at low flow and high flow conditions, pool 2 and riffle 2 immediately downstream, adapted from Caamaño *et al.*, (2009).

This specific site was selected for the detailed field data and numerical model output available for this reach. The site provides an opportunity to compare the numerically modeled flow structure (Caamano, 2008) with the laboratory observations, in addition to measuring the sediment transport behavior in the laboratory. The numerical model was calibrated against extensive field data, although there are no field observations for discharges above 80% of the bankfull discharge. Since most of the morphological changes occur at discharges at or greater than bankfull, the numerical simulations were used to scale the physical model.

### 3 METHODOLOGY

#### 3.1 Model Scale Computations

A Froude scaled physical model of the pool riffle sequence was constructed. A surface was created in ArcMap of the reach survey points. This surface was queried for bathymetric elevations every two meters for physical model construction. Figure 4 illustrates a 30 m by 60 m boundary drawn around the first pool-riffle sequence. The geometric length ratio ( $L_R$ ) between the model and prototype is:

$$L_R = \frac{L_P}{L_M} = \frac{30}{2} = 15 \quad (1)$$

$L_P$  = prototype or field length dimension (m)

$L_M$  = model length dimension (m)

$L_R$  = geometric length ratio

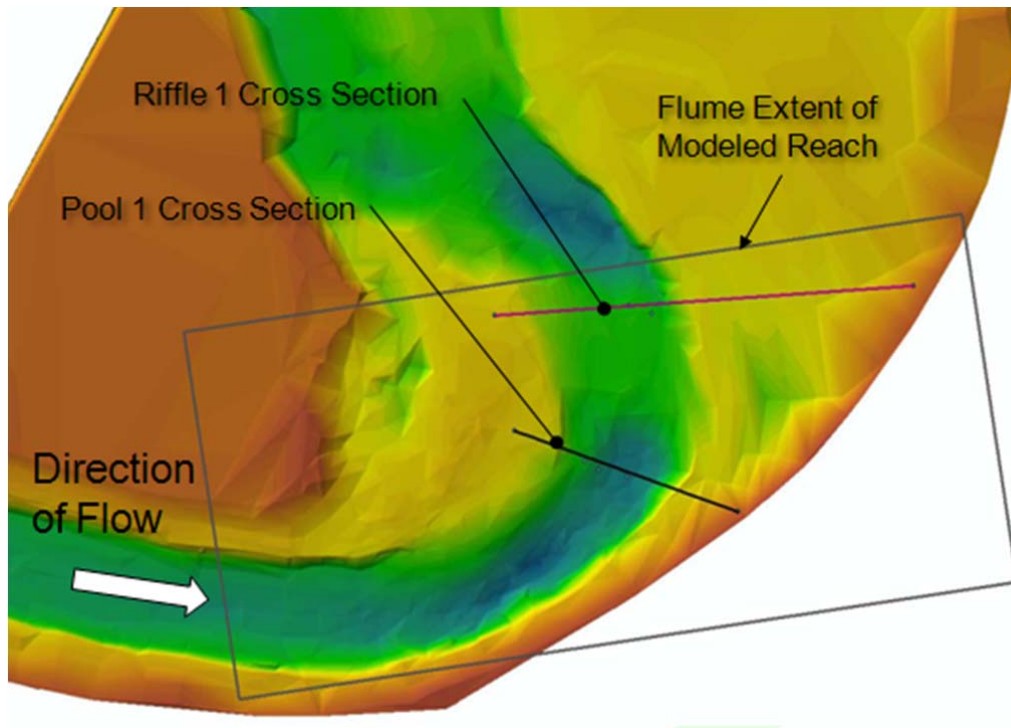


Figure 4. Generated surface using survey data with pool-riffle features identified within the modeled reach extent.

The pool and riffle cross sections are shown in Figure 5. The locations of these cross sections capture both the deepest point within the pool and across the riffle.

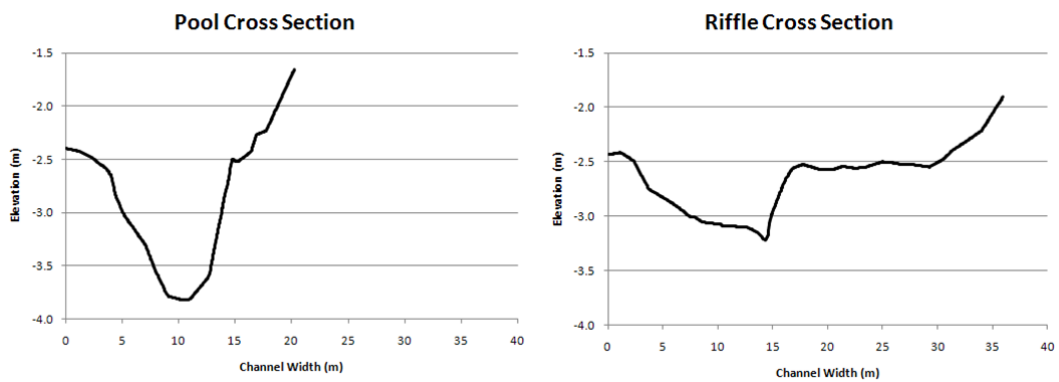


Figure 5. Plotted pool and riffle cross sections

In order for a physical model to be representative of the processes being evaluated, similarity between the significant model and prototype processes (or field conditions) must be retained,

although this is problematic for the sediment transport processes. The computations and assumptions that defined the representation of the modeled pool riffle sequence in the flume are summarized in Table 2. Turbulent flows were maintained in the model at all simulated discharges. The initiation of motion and sediment transport were analyzed using several approaches but the Shields criteria and the Meyer-Peter Mueller (MPM) sediment transport equations, shown in Table 2, were used to scale the particle sizes for the bathymetry used in this experiment. A lightweight artificial material was used in the experiments to represent bedload transport. Scaling the natural bedload sediment transport with lightweight artificial material resulted in larger particles that are not subject to cohesion and can be tracked visually. Nylon material was used, with a specific gravity of 1.15. Transport and initiation of motion were scaled on the basis of the average shear stress for the pool cross section which was estimated from the numerical model. Once the particle size was estimated, based on Shield's parameter for initiation of motion in the pool, two additional particles sizes were used to represent a larger and smaller diameter particle.

Table 2. Scaling parameters and ratios

Criterion	Equation	Scaled Ratio
Froude Number	$Fr = \frac{u}{\sqrt{gh}}$	$Fr_R = Fr_p / Fr_m = 1.0$
Reynolds Number	$Re = \frac{uh}{\nu}$ (733,000 prototype) (15,500 model)	$Re_R = Re_p / Re_m = 47.3$
Shear Stress	$\tau_b = \rho ghS$	$\tau_{bR} = \tau_{bp} / \tau_{bm} = 15.0$
Initiation of Motion (Shields Parameter)	$\theta_{cr} = 0.055$ (prototype material) $\theta_{cr} = 0.013D_*^{0.29}$ (model material)	$\Theta_{crR} = \Theta_{crp} / \Theta_{crm} = 1.0$
Dimensionless Particle Parameter	$D_* = \left[ \frac{(s-1)g}{\nu^2} \right]^{1/3} d_m$	$D_{*R} = D_{*p} / D_{*m} = 2.6$
Dimensionless Bed-load Transport Rate (MPM)	$\Phi_b = 8(\mu\theta - 0.047)^{1.5}$	$\Phi_{bR} = \Phi_{bp} / \Phi_{bm} = 1.0$
Volumetric Bed-load Transport Rate (MPM)	$q_b = \left( \sqrt{(s-1)g} d_m^{1.5} \right) \Phi_b$	$q_{bR} = q_{bp} / q_{bm} = 5.1$
Specific Gravity	$s_s = \frac{\rho_s}{\rho_w}$	$s_{s,R} = s_{s,p} / s_{s,m} = 2.3$

Table 3 presents the physical dimensions of the prototype pool riffle sequence and the modeled dimensions in the flume based on the geometric scaling ratio. The bank-full dimensions were based on numerical model results.

Table 3. Prototype and model dimensions at bankfull discharge

Calculated Physical Parameters		
	Prototype (Field)	Model (Flume)
Geometric Scaling	30 m width	2 m width
Pool		
Maximum Depth	1.64 m	0.11 m
Average cross sectional velocity	1.35 m/s	0.35 m/s
Riffle		
Maximum Depth	0.81 m	0.05 m
Average cross sectional velocity	1.29 m/s	0.33 m/s
Sediment		
Pool	17 mm	13 mm
$d_{transported}$ (computed size for movement)	13 mm	10 mm
	8 mm	6 mm

### 3.2 Model Construction

Model construction of the pool riffle bathymetry utilized natural sediments ranging in size from 3 mm to 8 mm and represented the scaled  $d_{50}$  to  $d_{90}$  material sampled in the pool. Observations during the past decade have shown that the larger sediment on the armored bed and bars move infrequently. Field measurements of bedload material transport taken with a Helley-Smith sampler indicate that the bed load transport material is considerably finer than the material found on the bed.

Due to the expected sensitivity of the results to bathymetry, particular care was taken in the accurate construction of the model. A grid frame was constructed within the flume representing 2 m spacing in the field and each intersection representing an elevation data point extracted from the ArcMap generated surface (Figure 6). Metal stakes were scored at 1 cm intervals to measure gravel depth and placed in a single row at each grid intersection. Once shaping and contouring of the bathymetry to the correct depths was completed, the grid points were painted and the stakes moved to the next row. Gravel was smoothed between each grid point and row to maintain a smooth transition between elevations. Once the entire grid was shaped, the elevations were verified prior to the model runs using an acoustic depth profiler and adjusted as nec-

essary. The approximate bankfull location of the water surface is painted on the model channel for documentation and reference purposes.

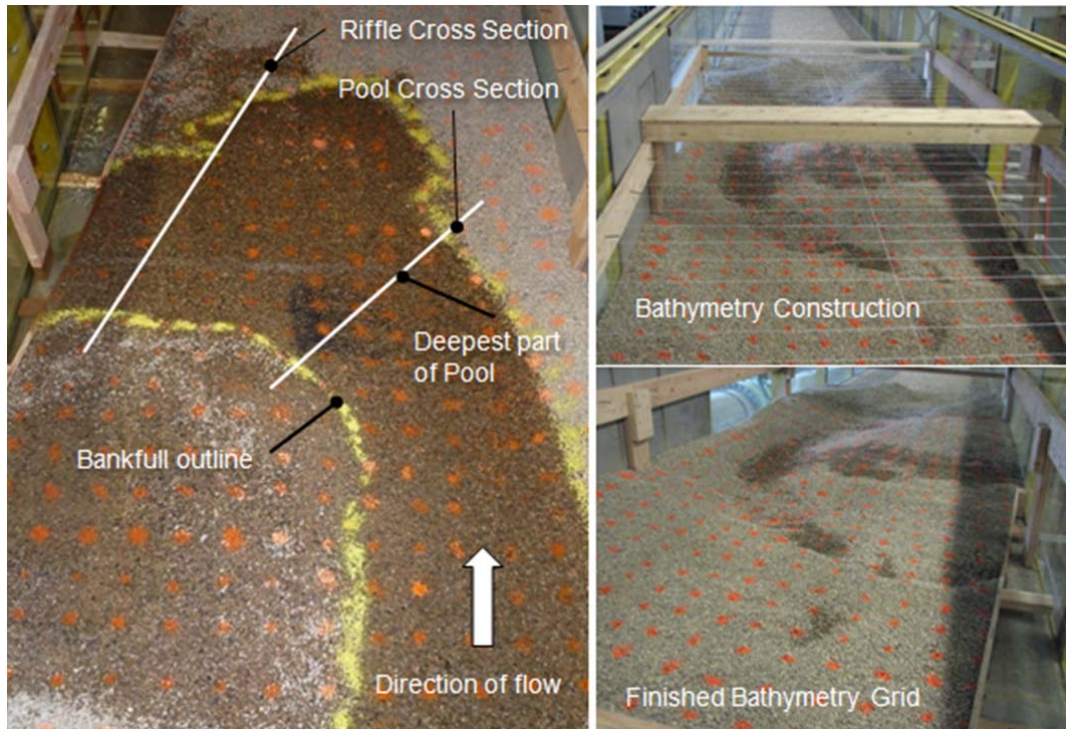


Figure 6. Flume construction of pool-riffle sequence and final configuration and location of cross sections

### 3.3 Model Scenarios

#### 3.3.1 Objectives

Numerical modeling of the pool-riffle sequence demonstrated a velocity reversal at bankfull conditions. At this discharge rate, the cross sectional velocity across the pool was greater than the riffle. The objectives of the physical modeling are to understand the spatial distribution of sediment flux reversal and the patterns of sediment deposition and erosion at a range of river discharges. These observations will then be used to assess the sustainability conceptual model postulated in Caamaño *et al.*, 2010.

The scenarios in the flume were developed with the following objectives:

1. Characterize the high velocity core formation at bankfull flows and greater, and validate the numerical modeling observations

2. Quantify when shear stress reversal occurs relative to velocity reversal
3. Quantify the point when sediment flux reversal occurs relative to velocity reversal
4. Characterize the formation of the high velocity core flow structure within the pool and how this changes when the pool begins to fill with sediment
5. Observe self-sustaining mechanisms within the pool-riffle sequence

Field observations and the predictions of numerical models indicate that significant bedload transport does not occur until the bankfull discharge is exceeded. The discharges used in the model are:

1. 110-percent bankfull discharge ( $1.1Q_{\text{BKF}}$ )
2. 120-percent bankfull discharge ( $1.2Q_{\text{BKF}}$ )
3. 135-percent bankfull discharge ( $1.35Q_{\text{BKF}}$ )
4. 145-percent bankfull discharge ( $1.45Q_{\text{BKF}}$ )

### 3.3.2 *High Velocity Core Visualization*

A dye tracer was employed to record the flow characteristics within the pool. Fluorescein dye was used with black light to enhance the visual contrast of the dye with the background. The grid points and bankfull line were visible under the fluorescent lights and provided dye release reference points for comparison between discharge scenarios. The dye injections were recorded to assess the presence and location of the flow features near and within the pool. The flow structure obtained from these images is compared qualitatively to the numerical model. The dye releases were made from an assembly consisting of a metal rod, syringe, and surgical tubing. It was configured such that the dye was released horizontally, into the flow stream, without interfering with the flow structure. Dye releases were made by hand to mimic local velocity conditions.

### 3.3.3 *Artificial Sediment Releases*

The artificial sediment was sized to be mobile at bankfull conditions and be representative of bedload sediment transport observed at the site. These sediments are either placed in the run upstream of the pool to observe the transport of bedload sediments into and through the pool, or the sediments were placed in the pool to observe the recovery or non-recovery of the pool morphology. Sediment movement was recorded as the flume was brought up to steady state discharge conditions and maintained for a defined period of time.

## 4 RESULTS

### 4.1 Velocity Characteristics

Dye tracer evaluation of the four discharge scenarios was performed. For presentation purposes, conditions representative of  $1.1Q_{\text{BKF}}$  and  $1.45Q_{\text{BKF}}$  are shown to demonstrate the extremes observed. Conditions observed at  $1.2Q_{\text{BKF}}$  and  $1.35Q_{\text{BKF}}$  followed the same trend between the discharges and, therefore, draw similar conclusions.

Figure 7 illustrates dye released at the pool's deepest location for two discharges. The left photograph depicts  $1.1Q_{\text{BKF}}$  while the photo on the right depicts  $1.45Q_{\text{BKF}}$  conditions. The near bed flow direction is directly across the point bar at the  $1.1Q_{\text{BKF}}$  discharge. Even though dye is released in the pool thalweg, it is diverted over the point bar to the left. A change in direction of the near-bed high velocity core flow was observed as the modeled flows were progressively increased. At the highest modeled discharge,  $1.45Q_{\text{BKF}}$ , the flow direction is maintained along the line of the pool thalweg and continues over the pool tailout toward the riffle.



Figure 7. Dye tracer visualization of flow direction at 1.1 times and 1.45 times bankfull conditions, respectively.

The visualizations demonstrate consistent flow patterns and behaviors observed in numerical model output or field measurements (Booker et al., 2001, Caamaño *et al.*, 2010). In these discussions, the term “jet” is used loosely to define the high velocity core structure generated by the physical attributes of the pool. Caamaño *et al.*, (2010) defined it as velocities greater than 90% of the maximum depth-averaged velocity observed within a cross section. Caamaño *et al.*, (2010) described the Coanda effect, the lateral pressure gradient across the pool, forcing the jet across the point bar, inside the bend (left photo, Figure 7) which was observed in the numerical simulations and at the field site. At higher flows, the high velocity core or jet migrates to align through the pool thalweg and toward the outer bank (right image).

Dye releases were made to identify and assess the eddy on the outside of the bend and high velocity core at different discharge conditions, features that had been observed from field measurements and numerical simulations (Figure 8). Thompson *et al.*, (1996) stated that these recirculating eddies, or wake zones, reduce the effective cross-sectional area of the pool, thus contributing to the area of higher velocity in the pool.

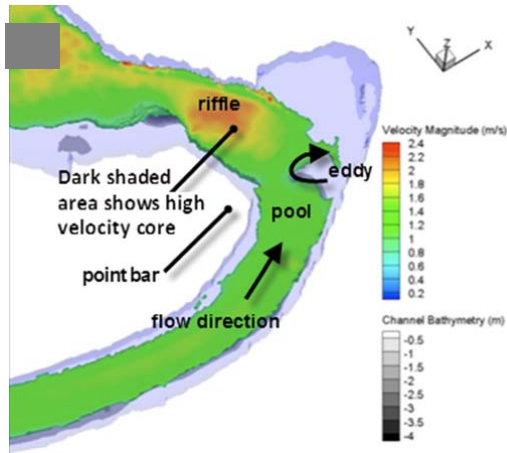


Figure 8. Numerical simulation of the high velocity core flow location of eddy feature (adapted from Caamaño, 2008)

Figure 9 illustrates the influence of the high velocity core on the eddy feature in these tracer studies. The images on the left are at  $1.1Q_{BKF}$  and the images on the right are  $1.45Q_{BKF}$ . The deepest part of the pool is marked with an “X” for reference. In the top images, dye is released upstream of the pool, near the bottom of the channel. The direction of the jet, as seen in Figure 9, migrates toward the outer bank as discharges increase. Superimposed is an arrow indicating the location of the eddy for comparison with the lower photographs. The lower photographs show the dye release in the eddy with the high velocity core or ‘jet’ direction superimposed. As discharges increased, the eddy feature remained present but became narrower in width and moved farther upstream. The persistence of the eddy feature at these high flows prevents the jet from impinging directly against the outer bank, thus reducing the opportunity for bank erosion.

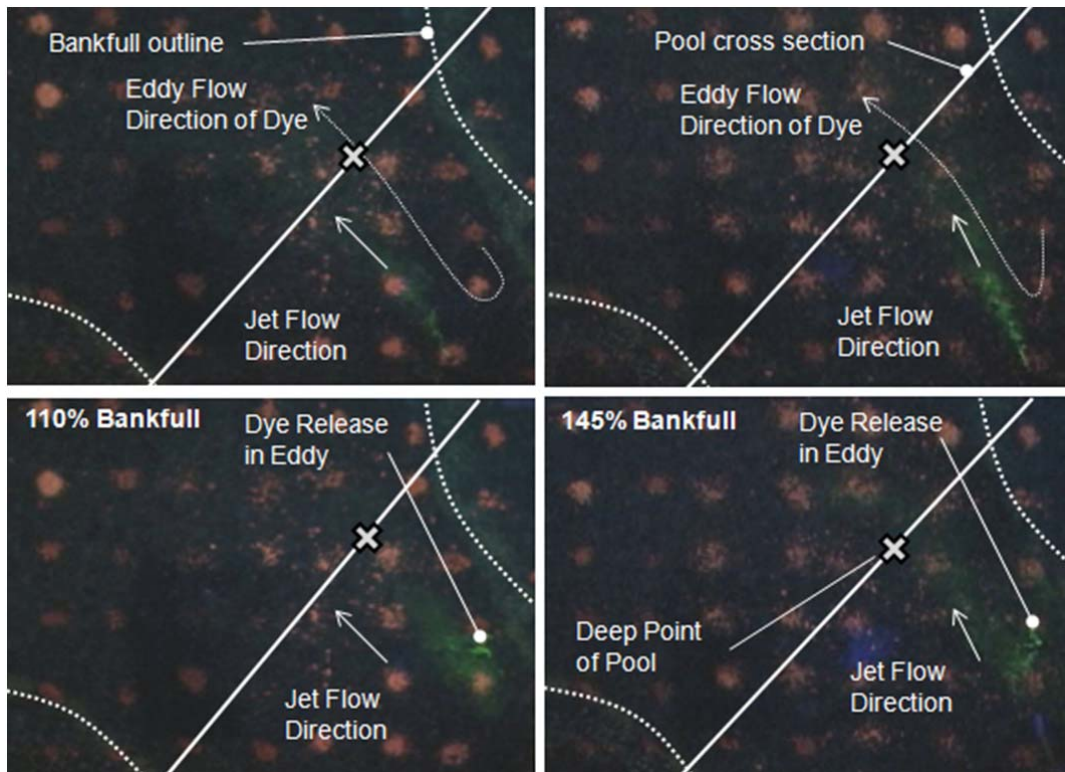


Figure 9. Stream bed dye releases upstream of the pool and within the eddy feature at  $1.1Q_{BKF}$  and  $1.45Q_{BKF}$

The results of the tracer studies provide a qualitative validation of the field observations and numerical simulations for this pool-riffle sequence.

#### 4.2 Shear Stress Reversal

In these experiments, the shear stress was evaluated through the initiation of motion of artificial sediment particles. The particle motion was observed for each series of constant discharges over 30 minutes. This period was selected based on scaling the duration of typical peak flood flows at the RRWMA. The  $1.2Q_{BKF}$  discharge was insufficient to scour the sediments in the deepest part of the pool, although a few particles did move onto the riffle. However at  $1.45Q_{BKF}$ , most of the deposited sediment was scoured from the bottom of the pool and was either deposited on the riffle or was transported out of the study reach. This implies that for this pool-riffle sequence, the shear stress reversal occurs between 1.2 and  $1.45 Q_{BKF}$ . The dye studies indicate that this was also the flow range where the high velocity core realigned from across the point bar to follow the thalweg. The scour of sediments from the deepest part of the pool

and subsequent deposition onto the downstream riffle demonstrate the process that sustains the pool and builds the riffle crest (Figure 10). The black dotted line shows the deepest part of the pool and the initial location of the sediments and the solid black line highlights the area of particle deposition.

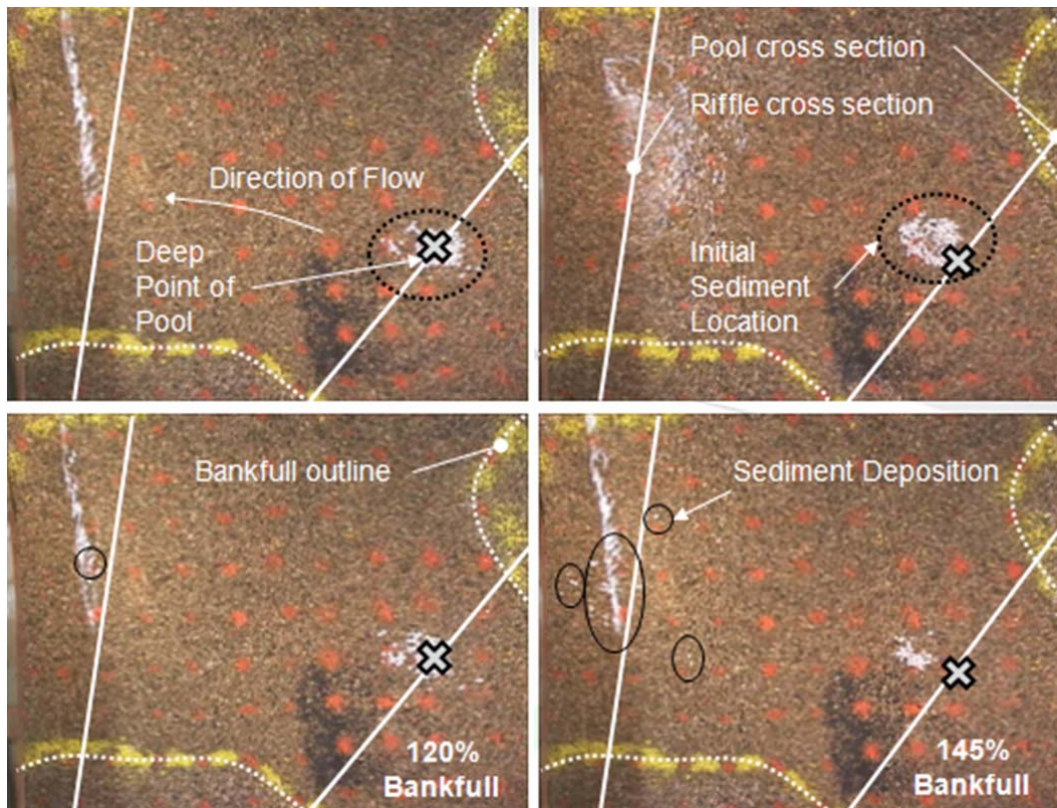


Figure 10. Sediment scour from pool at  $1.2Q_{BKF}$  and  $1.45Q_{BKF}$

Table 4 summarizes the fate of the marked particles in the deepest part of the pool for each discharge.

Table 4. Scour and deposition of particles from the pool thalweg

Shear Stress Results			
Discharge Rate	Deposition Location		
	Pool or Pool Tail Out	Riffle	Particles moving out of reach
1.1 $Q_{BKF}$	0%	0%	0%
1.2 $Q_{BKF}$	99%	1%	0%
1.35 $Q_{BKF}$	58%	33%	9%
1.45 $Q_{BKF}$	40%	26%	34%

The average shear stress through the pool and riffle were estimated from the water surface elevation slope observed in the physical model and the results are normalized with the bed shear stress calculated at  $Q_{1.1BKF}$  (Figure 11). The small scale of the model resulted in some inaccuracy in the estimation of water surface slope, but the trends and relative differences between discharges are consistent. The estimates of low flow shear stress were made using field measurements.

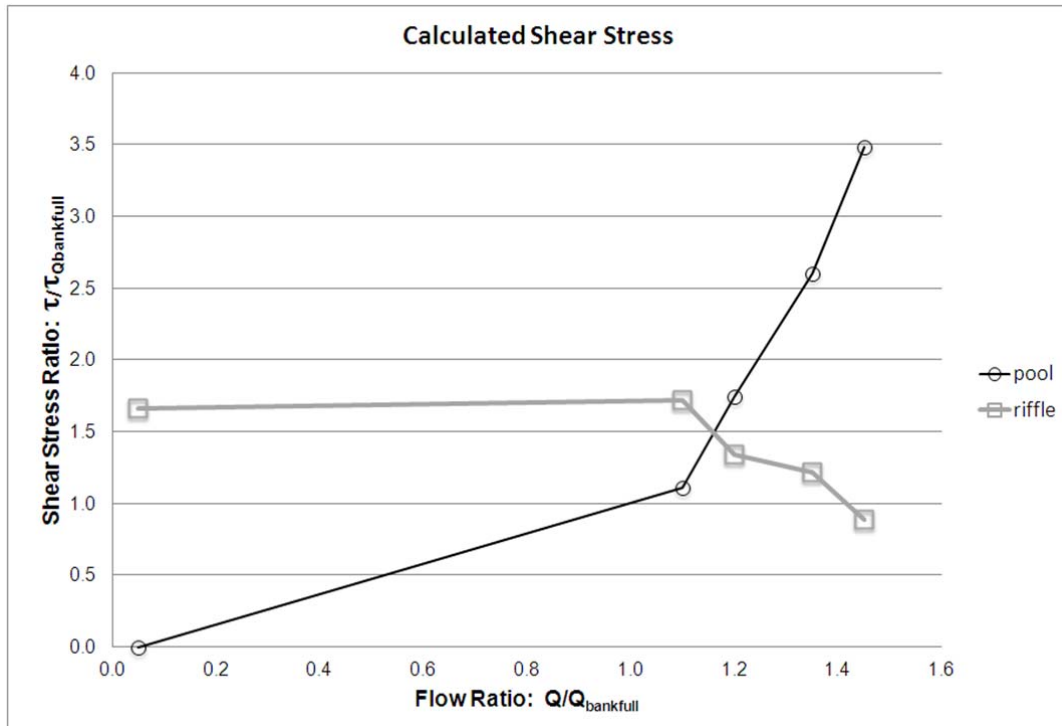


Figure 11. Estimate of normalized average shear stress reversal from the physical model.

The trend toward shear stress reversal was also evident in the numerical simulations (Caamaño, 2008). The shear stress was computed utilizing both the quadratic stress law and the logarithmic velocity relationship. Both methodologies indicated a reduction of the riffle shear stress between the medium flow and bankfull flow modeled. That trend also indicated that reversal should occur at discharges greater than bankfull. The decrease in riffle shear stress as the discharge increases could be attributable to downstream control affecting this upstream pool-riffle sequence (De Almeida & Rodriguez, 2011, Caamaño, 2008). This indicates that the occurrence of shear stress reversal could be influenced by both downstream control and the local bathymetry.

#### 4.3 Sediment Flux Reversal

These scenarios assess sediment flux reversal by quantifying the relative difference between the pool and riffle bed load transport. The artificial sediment particles were aligned across the run, just upstream of the pool and simulate the fate of bedload moving through the reach at high discharges (Figure 12). Flow was gradually increased until the target discharge was achieved and then held constant for 30 minutes. For all of the modeled discharges, none of the mobilized particles deposited within the pool. The sediments were transported through the pool and either deposited on the riffle, point bar, or continued out of the study reach (Table 5). Another observation was that as the modeled discharges increased, deposition on the point bar occurred higher up the bank. In addition, more sediment was deposited on the riffle than carried downstream. These results demonstrate that at discharges higher than bankfull, sediment flux, or bedload transport, through the pool is greater than across the riffle. Mobilization of the bedload sediments did not occur until  $1.2Q_{BKF}$ , therefore, sediment flux reversal may occur near bankfull for smaller sediments than those represented in these experiments.

These sets of experiments provided validation of the sediment flux reversal occurring for this pool-riffle sequence. The numerical model results of this sequence also indicated that near bankfull, reversal would occur although there is considerable uncertainty in the sediment transport formula used for simulating localized differential transport (Caamano, 2008). These results also show the incoming sediment particles are building the point bar and riffle, not filling the pool.

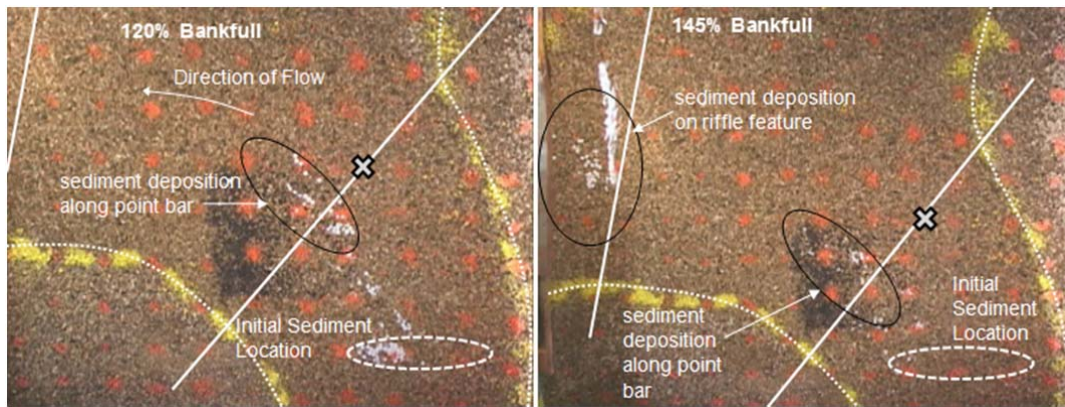


Figure 12. Transport of artificial sediment at  $1.2Q_{BKF}$  and  $1.45Q_{BKF}$  discharges

Table 5. The deposition of incoming particles in the study reach at high flows

Sediment Flux Results			
Discharge Rate	Deposition Location		
	Point Bar	Riffle	Out of System
$1.1Q_{BKF}$	0%	0%	0%
$1.2Q_{BKF}$	94%	4%	2%
$1.35Q_{BKF}$	85%	11%	4%
$1.45Q_{BKF}$	55%	29%	17%

#### 4.4 Pool Infill

The preceding scenarios described the scour and deposition trends of sediments for the current channel morphology. Although this morphology has been stable for the past decade, it is possible that under a different sequence of annual hydrographs that sediment could have accumulated within the pool through either the lack of large flows capable of scouring the pool or an overload of sediment to the system due to changing landuse practices or the consequences of wild-fire in the basin. These scenarios evaluate the ability of the pool to recover following the accumulation of significant sediment in the pool. The sedimentation in the pool assumed that the sediment delivery to the study reach had exceeded the bedload transport capacity of the pool for some period of time. The visualizations of the flow characteristics were made to assess the potential recovery mechanisms. The pool feature was in-filled to approximately 90-percent of the residual pool depth to compare the numerical simulations of the same condition (Caamaño *et al.*, 2010).

#### 4.4.1 Flow Characteristics

The dye tracer technique was used to compare pool features under in-filled and original conditions. Dye was released across the surface of the pool feature from river left to right at a flow condition of  $1.1Q_{BKF}$ . For existing conditions, the eddy on the outer bank is very pronounced (Figure 13, left image). When the pool is filled with sediments, the eddy is no longer present. Without the eddy feature, the dye directly impacts the outer bank. This validates the numerical model output observations under the similar discharge conditions.

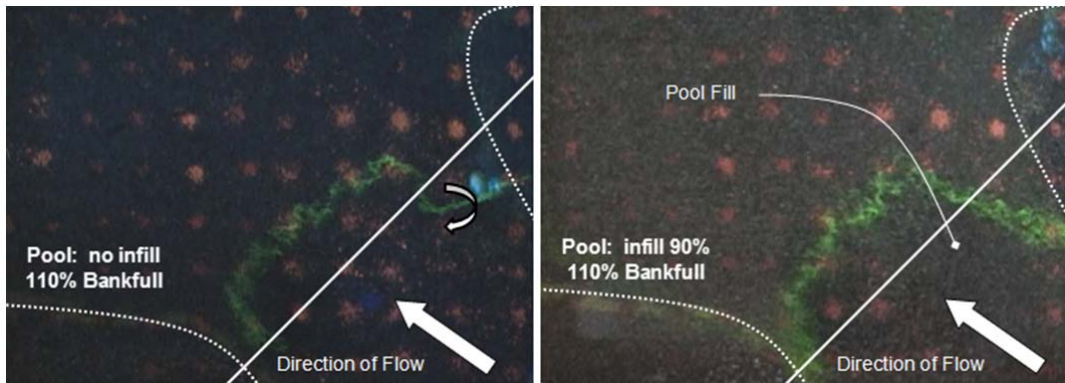


Figure 13. Dye tracer comparison between original pool structure and infilled condition.

When dye was released upstream of the pool, the distinct high velocity core is more diffuse in the infilled pool (Figure 14, right image). Even with remnants of the point bar in place, there is not enough constriction of the flow to create the high velocity core or any large eddies.

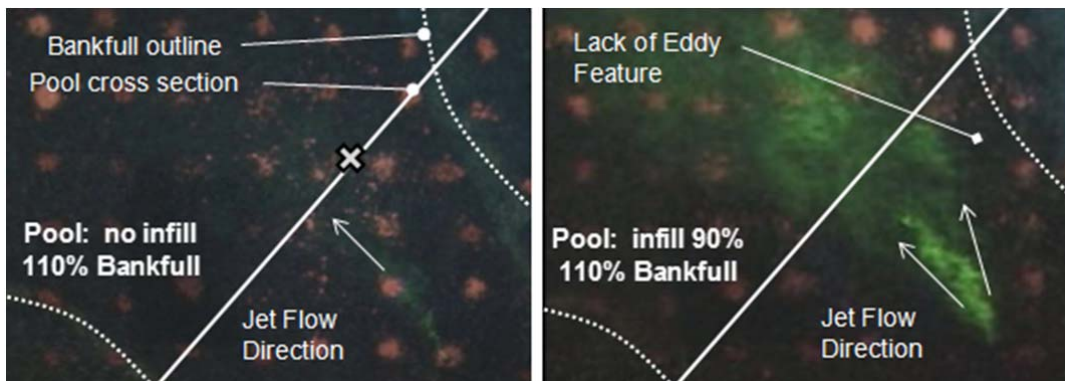


Figure 14. Dye tracer comparison of jet formation between original pool structure and infilled condition

#### 4.4.2 Pool Recovery

Artificial sediment particles were placed on top of the pool infill area at the former deepest part of the pool to assess their mobility and potential for pool recovery by scour. Very little movement of the particles occurred and the few particles that did move were transported downstream and were not deposited preferentially on the riffle or point bar. Figure 15 illustrates the location of the sediments after 15 minutes at  $1.45Q_{BKF}$ . Similar to the numerical model results, at bank-full conditions, shear stress reversal was not observed and this condition potentially indicates a situation where pool recovery may not be possible.

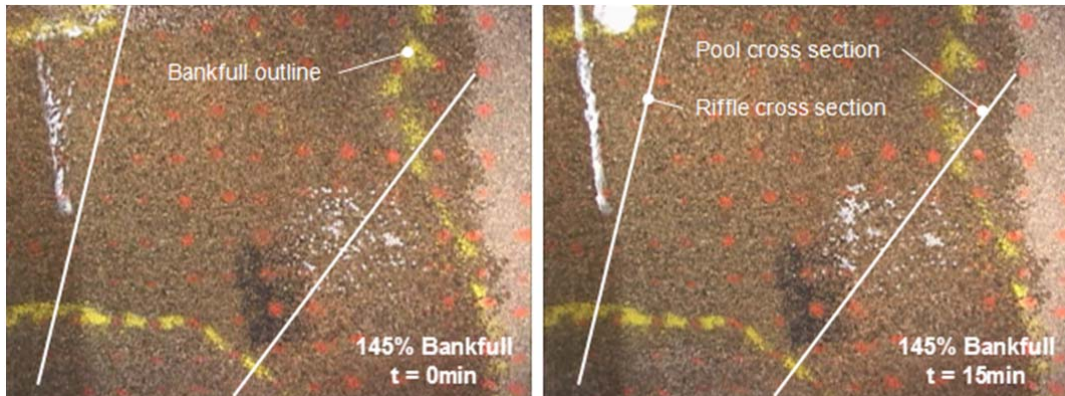


Figure 15. Artificial sediment movement on top of pool in-fill section at  $1.45Q_{BKF}$

However, if bedload transport occurs, there may be an alternative mechanism for recovery. Sediments were placed across the run, just upstream of the in-filled pool section. The discharge of  $1.45Q_{BKF}$  was held constant for 30 minutes. The sediments were deposited toward the upstream end of the point bar and began to elongate the bar (**Error! Reference source not found.**Figure 16). Under these circumstances, if the point bar develops at a faster rate than erosion of the outer bank, the semblance of a jet feature may gradually redevelop. Eventually the point bar will constrain the flows and possibly scour the sediments that had filled the pool or will create a constriction capable of forming a new pool. The key factor would be whether the outer bank would erode faster or keep pace with the build out of the point bar. If the bank erodes such that the reduction in pool width compared to the riffle cannot be generated, then the pool will be unable to recover.

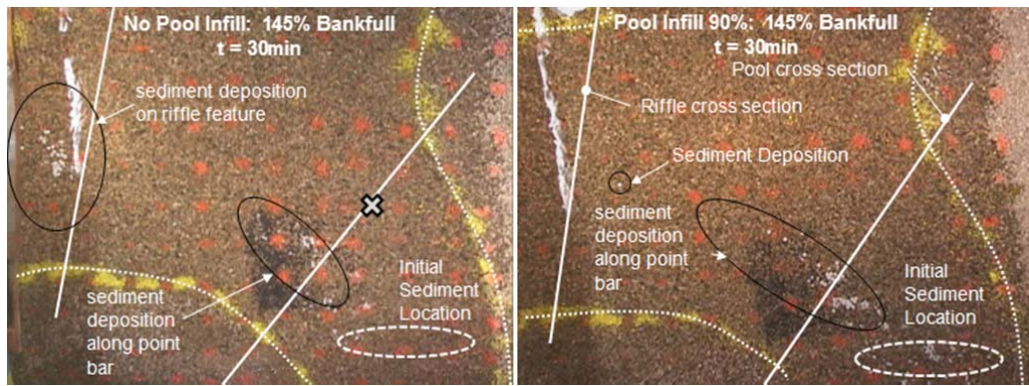


Figure 16. Comparison of sediment flux between the original pool configuration and the infilled pool.

## 5 CONCLUSION

### 5.1 Flume Model

Dye tracer analysis qualitatively validated the general behavior of the high velocity core feature predicted by numerical studies. As discharges increased above bankfull, the jet direction migrated from the inner bank, across the point bar towards the outer bank. The existence of an eddy feature on the outer bank was present at flows greater than bankfull. The eddy prevented direct impact of the high velocity core against the outer bank. As flows increased above bankfull, the jet orientation begins to align through the pool thalweg and the sediments begin to scour out of the pool. These sediments deposit in the pool tail out, the riffle, or carried further downstream. This phenomenon was also witnessed in a forced pool configuration (MacVicar & Roy, 2010) where flow acceleration due to the constriction mobilized the sediments in the center of the pool and over the exit slope.

The artificial sediments representing the coarse bedload placed upstream of the pool were not mobile until roughly  $1.2 Q_{BKF}$ . When mobilized, none of the sediments deposited within the pool, most likely due to entrainment in the jet turbulence (MacVicar & Roy, 2007) and carried around the deep part of the pool. Some of the sediments were carried out of the study reach while some of the entrained sediment deposited directly on the downstream riffle. Deposition also occurred along the point bar as sediment was routed over the side bar near the pool entrance. MacVicar & Roy (2010) also documented this sediment deposition characteristic at their forced pool-riffle study site. As the flows increased, deposition of the sediments occurred higher up on the bar. It is also interesting to note that deposition percentage on the riffle was greater than the percentage of sediments carried out of the study reach. Based on these observations, it can be surmised that sediment flux reversal occurs at flows greater than bankfull conditions and

the transport characteristics observed are the primary processes for sustaining the pool morphology.

The pool feature was filled with pea-gravel bed material to approximate the numerically modeled 90-percent infill condition (Caamaño *et al.*, 2010). The dye tracer analysis validated the numerical model output and demonstrated that the eddy feature was no longer present to protect the outer bank. In addition, the lack of a defined high velocity core or jet was also apparent in the visualizations. Artificial sediment deposited across the in-filled pool did not mobilize at any of the modeled discharges. This indicates that the high velocity core structure plays a role in pool maintenance. The scenario simulating the fate of bedload material being transported into the study reach when the pool is filled indicated the possibility of elongating the point bar. If the building of the point bar occurs at a faster rate than outer bank erosion, it is possible that the constriction necessary to create the pool riffle morphology could develop over time, but this process would be slower than scouring the pool fill material.

## 5.2 Conceptual Model

A conceptual model for self-sustaining pool-riffle features was developed in Caamaño *et al.*, (2010) utilizing field data and other observations (Dietrich & Smith, 1984, MacWilliams *et al.*, 2006, Pasternack *et al.*, 2008). The preliminary results from this physical modeling exercise further clarify the various principles postulated in the conceptual model.

1. The physical model demonstrated that near bankfull conditions, a sediment flux reversal occurred, preserving the pool feature and depositing material along the point bar or riffle. This assumption is predicated on the fact that the sediment flux transport of the pool exceeds that of the sediment delivery to the study reach.
2. If the pool was not aggraded to a point where a jet structure was no longer present, local transport capacity was exceeded and the pool could scour. Higher than bankfull flows were necessary to redirect the high velocity core from the point bar to the pool thalweg. At all the modeled discharges, the eddy feature was present and provided a level of protection to the outer bank.
3. A scenario modeled in the flume considered the altered flow structure and scouring ability if sediment accumulated in the pool and reduced the residual pool depth to 10% of the existing bathymetry. In this condition the well-defined high velocity core was no longer present. The eddy feature was also gone and the high velocities directly impacted the outer bank.

4. Artificial sediments placed in the in-filled pool were not mobilized under any of the modeled discharges. It was also shown that sediment transported into the study reach is routed across the side bar upstream of the pool. While the sediments were not entrained and carried to the riffle and deposited, they did create an elongated point bar. Therefore, if a flow constriction could begin to form near the top of the pool, and if the point bar formed faster than the rate of outer bank erosion, then a jet could gradually develop. If this occurred, it is possible that the pool feature could re-form.

## 6 ACKNOWLEDGMENTS

The original concept of the study was developed by Dr. Gerhard Jirka and the authors with the intent of supporting collaborative research between the University of Idaho and Karlsruhe Institute of Technology through exchange visits. These preliminary results of the physical model study are presented as a tribute to Dr. Jirka and his commitment to exploring innovative applications of fluid mechanics to environmental issues, for supporting young professionals and fostering international collaboration. The authors would like to acknowledge the support of Reclamation's Pacific Northwest Region through Reclamation's Science and Technology Program (Grant ID 4362) to investigate pool-riffle sustainability mechanisms. Reclamation's Columbia Snake Salmon Recovery Office (CSRO) receives federal monies to improve and restore salmonid habitat impacted by the construction of federal dams. These mitigation efforts include the design of specific habitat features for several lifestages of salmonids in various streams or rivers identified throughout the Northwest. This publication was made possible by the NSF Idaho EPSCoR Program and by the National Science Foundation under award numbers EPS-0814387 and BES-9874754) as well as the Chilean Fondecyt Project N° 11100399.

## 7 REFERENCES

- Booker, D. J., Sear, D. A., and A.J., P. (2001). Modeling three-dimensional flow structures and patterns of boundary shear stress in a natural pool-riffle sequence." *Earth Surface Processes and Landforms*, 26, 553-576.
- Caamaño, D., Goodwin, P., Buffington, J.M. (2010) Flow structure through pool-riffle sequences and a conceptual model for their sustainability in gravel-bed rivers. *River Res. Applic.* [Online] Available from doi:10.1003/rra. 1463 [Accessed May 2011].

- Caamaño, D., Goodwin, P., Buffington, J.M., Liou, J.C., Daley-Laursen, S. (2009) A unifying criterion for velocity reversal hypothesis in gravel-bed rivers. *Journal of Hydraulic Engineering*. ASCE. 135(1). 66-70.
- Caamaño, D (2008). The velocity reversal hypothesis and implications to the sustainability of pool-riffle bed morphology (Doctoral dissertation). Boise, Idaho, University of Idaho.
- De Almeida, G.A M., & Rodriguez, J.F. (2011) Understanding pool-riffle dynamics through continuous morphological simulations, *Water Resour. Res.*, 47. W01502.
- Dietrich, W.E., and Smith, J.D. (1984). Bed Load Transport in a River Meander, *Water Resour. Res.*, 20(10), 1355-1380.
- Federal Interagency Stream Corridor Restoration Working Group, (1998). Stream Corridor Restoration: Principles, Processes, and Practices. By the Federal Interagency Stream Restoration Working Group (FISRWG)(15 Federal agencies of the US government). GPO Item No. 0120-A; SuDocs No. A 57.6/2:EN 3/PT.653. ISBN-0-934213-59-3. [http://www.nrcs.usda.gov/technical/stream\\_restoration/](http://www.nrcs.usda.gov/technical/stream_restoration/)
- Garcia, M.H. (2008) "Sediment Transport and Morphodynamics". *Sedimentation Engineering: Processes, Measurements, Modeling, and Practice*. No. 110. ASCE. New York N.Y.
- Gilbert, G. K. (1914). "The transportation of debris by running water." *US Geological Survey Professional Paper* 86, Washington, D.C.
- Keller, E. A., and Florsheim, J. L. (1993). "Velocity-reversal hypothesis: A model approach." *Earth Surface Processes and Landforms*, 18, 733-740.
- Klein, L.R., Clayton, S.R., Alldredge, J.R., and Goodwin, P. (2007). Long-term monitoring and evaluation of the Lower Red River Meadow Restoration Project, Idaho, U.S.A. *Restoration Ecology*, 15, 2, 223-229.
- Knighton, D. (1998). *Fluvial Forms & Processes: A new perspective*, Arnold, London.
- Leopold, L. B., Wolman, M. G., and Miller, J. P. (1964). *Fluvial Processes in Geomorphology*, Freeman, San Francisco.
- Lisle, T. E. (1982). Effects of aggradation and degradation on riffle-pool morphology in natural gravel channels, Northwestern California." *Water Resources Research*, 18(6), 1643-1651.
- van Rijn, L.C. (1993) *Principles of Sediment Transport in Rivers, Estuaries and Coastal Seas*. Amsterdam, Aqua Publications.

- MacVicar, B.J., and A.G. Roy (2007). Hydrodynamics of a forced riffle pool in a gravel bed river: 1. Mean velocity and turbulence intensity. *Water Resour. Res.*, 43. W12401.
- MacVicar, B.J., and A.G. Roy (2007). Hydrodynamics of a forced riffle pool in a gravel bed river: 2. Scale and structure of coherent turbulent events. *Water Resour. Res.*, 43. W12402.
- MacWilliams, M.L., Jr., J.M. Wheaton, G.B. Pasternack, R.L. Street, and P.K. Kitanidis (2006) Flow convergence routing hypothesis for pool-riffle maintenance in alluvial rivers, *Water Resour. Res.*, 42. W10427
- Montgomery, D.R., Buffington, J.M., Smith, R. Schmidt, K., Pess, G. (1995). Pool spacing in forest channels. *Water Resour. Res.*, 31:1097-1105.
- Pasternack, G.B., Bounrisavong, M.K., Parikh, K.K. (2008). Backwater control on riffle-pool hydraulics, fish habitat quality, and sediment transport regime in gravel-bed rivers. *Journal of Hydrology* 357: 1-2: 125-139.
- Pugh, C.A. (2008). "Sediment Transport Scaling for Physical Models". *Sedimentation Engineering: Processes, Measurements, Modeling, and Practice*. No. 110. ASCE. New York, N.Y.
- Richards, K. S. (1976). The morphology of riffle-pool sequences. *Earth Surface Processes and Landforms*, 1, 71-88.
- Stanford, J.A., Lorang M.S., and Hauer F.R. (2005). The Shifting Habitat Mosaic of River Ecosystems. *Verh. Internat. Verein. Limnol.*, 29. 123-136.
- Thompson, D.M. (2011). The velocity-reversal hypothesis revisited, *Progress in Physical Geography*, 35: 123.
- Tilman, D. (1999). The ecological consequences of changes in biodiversity: a search for general principles. *Ecology*, 80, 1455-1474.
- Wilkinson, S. N., Keller, R. J., and Rutherford, I. D. (2004). "Phase-shifts in shear stress as an explanation for the maintenance of pool-rifle sequences." *Earth Surface Processes and Landforms*, 29, 737-753.
- Wohl, E. E. (2000). *Mountain Rivers*, American Geophysical Union, Water Resources Monograph, Washington, DC.